Available online at www.sciencedirect.com

ScienceDirect

Procedia CIRP 95 (2020) 731–736

www.elsevier.com/locate/procedia

20th CIRP CONFERENCE ON ELECTRO PHYSICAL AND CHEMICAL MACHINING

Experimental study on the mitigation of surface damages caused in electrochemical discharge machining of glass

Yu-Jen Chen, Murali Sundaram*

Department of Mechanical and Materials Engineering, University of Cincinnati, Cincinnati, OH, USA

* Corresponding author. Tel.: +1-513-556-2791; fax: +1-513-556-3390. *E-mail address:* murali.sundaram@uc.edu

Abstract

Electrochemical discharge machining (ECDM) is an emerging method suitable for the micromachining of nonconductive materials such as glass. ECDM is a hybrid process in which material removal involves both chemical and thermal mechanisms. Various process parameters affect the performance of ECDM. Improper ECDM working conditions may lead to undesirable surface damages in glass machining. This paper investigates the methods to mitigate surface wrinkle formation caused by the chemical mechanism and surface cracks caused by the thermal mechanism in the ECDM machining of borosilicate glass. ECDM in an acidic environment was found to avoid surface wrinkling caused by chemical etching in glass machining. Moreover, both thermal and chemical damages are mitigated when ECDM was performed with a mixed electrolyte.

Keywords: ECDM; Glass; Micromachining; Surface analysis; Thermal effects;

1. Introduction

Electrochemical discharge machining (ECDM) is an emerging nontraditional process wherein material removal could happen due to anodic dissolution, as well as spark erosion [1]. Thus, ECDM has the unique ability to machine non-conductive materials [2-4]. In this process, also known as the spark assisted chemical engraving (SACE) [5], typically a small cathode (usually the tool electrode) and relatively a larger anode are immersed in an electrolyte tank with the workpiece kept separately just beneath the cathode. When the applied voltage exceeds the critical voltage, electrical discharges occur between the tool and the surrounding gas film to cause material removal. The cause of gas film formation is often attributed to the coalescence of hydrogen bubbles produced by the electrolysis [5-7] and also to the Joule heating of the electrolyte [8-11]. The gas film formation by the coalescence of hydrogen bubbles is studied using the percolation theory [6].

As the gas bubbles accumulate around the tool, the resistance in the gap of the gas bubbles would drastically increase. That is, the effect of Joule heating would increase the temperature and cause vaporization which would also form of the gas film [10, 11]. Therefore, both the hydrogen bubbles and Joule heating could possibly contribute to the formation of the gas film. It is interesting to note that the gas film in ECDM often contains more elements than just hydrogen [5]. Especially when sodium hydroxide or potassium hydroxide is used in ECDM, ions of sodium or potassium were found in the gas film. These ions in the gas film can be an important factor for discharges and material removal. The material removal in ECDM is a complex process wherein different effects simultaneously occur. This includes the thermal machining caused by the high temperature, of the sparks, and the chemical etching process. This chemical effect increases the material removal rate but also causes noticeable wrinkling surface damage.

10.1016/j.procir.2020.02.257

Wrinkling can be reduced by lowering the concentration of the electrolyte [12], but total elimination needs minimization of chemical reactions. The thermal damages such as cracks are attributed to the Joule heating and the high local temperature of the sparks. The intensity of the spark can be affected by many factors such as the voltage (e.g., the energy of the spark) or the element of the electrolyte. Varies studies have shown the effect of different electrolyte which would affect the material removal and thermal damages [10, 13-15]. It has been shown that KOH and NaOH have a much higher material removal rate (MRR) than acids due to their chemical machining. On the other hand, machining with sulfuric acid has been found to have a higher chance to break the glass workpieces [13]. A few other studies have reported that the color and light intensity of the spark can vary in different electrolytes [13, 16, 17]. In these studies, the ions in the electrolyte were noticed to be a major element causing the variety of colors in sparking. For example, H_2SO_4 is reported to spark in a blue color [13], and KOH caused purple sparks [16]. Thus, it has been reported that the color of the ECDM discharge varies in electrolytes with different ions. The color of sparking was found to affect the thermal damage of the machining material. Also, a mixture of electrolytes with multiple ions was demonstrated which moreover reveals the effect of different ions in the electrolyte. Thus, by controlling the composition of the electrolyte, it is hypothesized that the spark color and the machining environment (i.e., avoiding undesired chemical reaction) can be adjusted to reduce the damages of the surfaces machined in the ECDM process.

2. Experimental method

Figure 1 shows the in-house built ECDM experimental setup used in this study. This setup includes a DC power supply (0-120 V) a current probe connected to LabView for data acquisition and analysis. The gas bubbles and gas film were observed by a high-speed camera. Details of the experimental parameters used in this study are listed in Table 1.

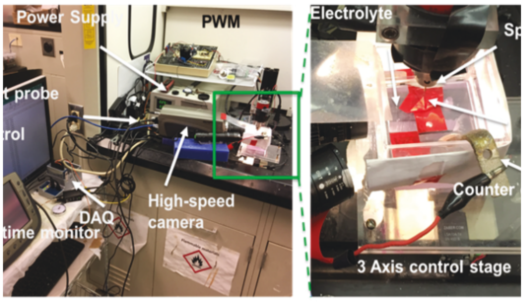

Figure 1. The in-house built experimental setup.

Table 1. Parameters for the ECDM machining.

Parameters	Values
Work Piece	Borosilicate glass
Tool	1 mm cylinder WC
Applied voltage	45 V DC
Electrolyte	NaOH, H2SO4, HCl, KOH, mixture
Electrolyte level	
Tool rotation speed	1200 rpm
Machining time	1 minute

The electrolyte level is selected at 3 mm for the least thermal damage [18]. A tool rotation is applied to decrease the thermal damage caused by energy concentration. The machined surfaces were studied with an optical and scanning electron microscopes.

3. Results and discussion

3.1 Effects of electrolyte temperature

Figure 2 shows the current data acquired in ECDM performed 2 M NaOH at room temperature (25 ºC). Three distinct phases namely, an unstable stage, an electrolysis stage, and a continuous sparking stage can be observed from the current signal. In the initial unstable stage, from 0 to less than 0.1 s, the current starts to decrease due to the coverage of the gas bubble at the surface of the tool. Then, the current dropped to a close-to-zero value which means that the gas bubble has a near total coverage of the tool. At this stage, this unstable large gas bubble collapsed leading to the resumption of electrolysis.

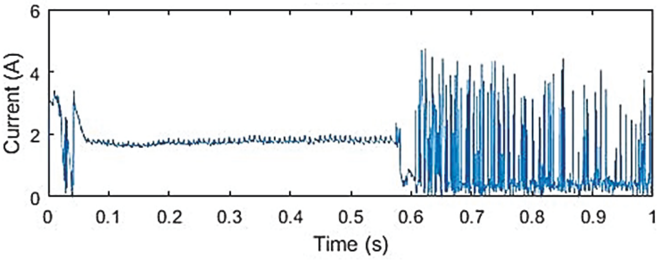

Figure 2. The current signal for the first second of ECDM with 2 M NaOH at 45 V, 25 ºC.

Figure 3 shows the corresponding high-speed camera images of the gas film formation process. In the electrolysis stage (i.e., after the unstable stage but before sparking occurs), no gas film formation or sparking was found. The bubble was noticed to be small and uniformly covering the tool, as the larger bubble would flow towards the surface of the electrolyte. For example, the gas bubble would look similar from 0.06 s to 0.6 s (i.e., Figure 3 (d) to (e). Finally, these gas bubbles will start to coalesce into a more stable gas film. At this time (after 0.6 sec), the third phase i.e. the continuous sparking begins.

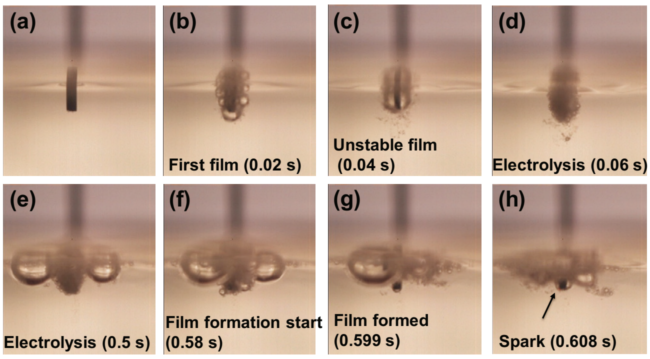

Figure 3. High-speed camera images of the gas film formation process corresponding to data in Figure 2. An unstable gas film was formed at the start of the process (first row). After approximately a 0.5 s electrolysis, another more stable gas film is formed and starts sparking (second row).

The pure electrolysis phase was not observed after the sparking process begins. The gas film formation in this phase is probably aided by the evaporation of the electrolyte caused by the Joule heating effect. As the current flows through the electrolyte, the temperature would increase. As the temperature continuously increasing the electrolyte would vaporize and merge with the hydrogen gas bubbles generated from the electrolysis to form the gas film. This assistance of vaporized electrolyte advances the gas film formation process to occur at a smaller gas bubble size, which can be expected to result in the formation of a thinner gas film. The thickness of the gas film can be compared between Figure 3 (c) and (g) (i.e., unstable, and stable gas film). Surface wrinkling caused by chemical effects can be seen in the optical image (Figure 4) of the glass surface machined in this condition.

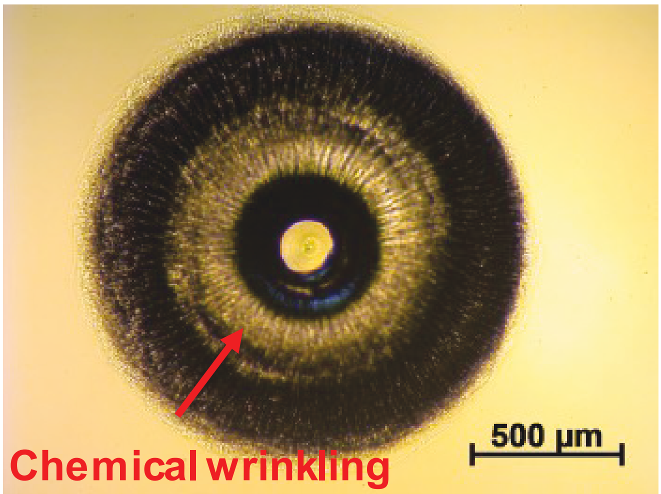

Figure 4. Machined surface for 2 M NaOH at 45 V at 25 ℃.

In order to reduce the chemical wrinkling, it is required to reduce the electrolysis period. For this purpose, the temperature of the electrolyte was increased to 50 ℃. By increasing the temperature, the electrolysis stage was noticed to be much shorter than at 25 ℃. as shown in Figure 5.

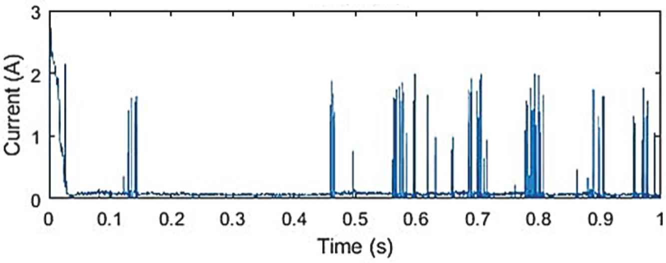

Figure 5. The current signal for the first second of ECDM with 2 M NaOH at 45 V, 50 ℃.

By increasing the initial electrolyte temperature, the total time before the continuous sparking is much shorter. It was observed that the current and sparking density is reduced by increasing the electrolyte temperature from 25 ℃ to 50 ℃ (compare Figure 2 with Figure 5). This can be understood as that the gas film thickness is reduced by increasing the electrolyte temperature.

The machining results in Figure 6 does show that the wrinkling density has reduced, and the hole diameter is slightly smaller compared with the machining at 25 ℃. However, the wrinkling is still not eliminated. Therefore, the alternate approach i.e. changing the ions in the electrolyte was attempted to reduce the surface damages.

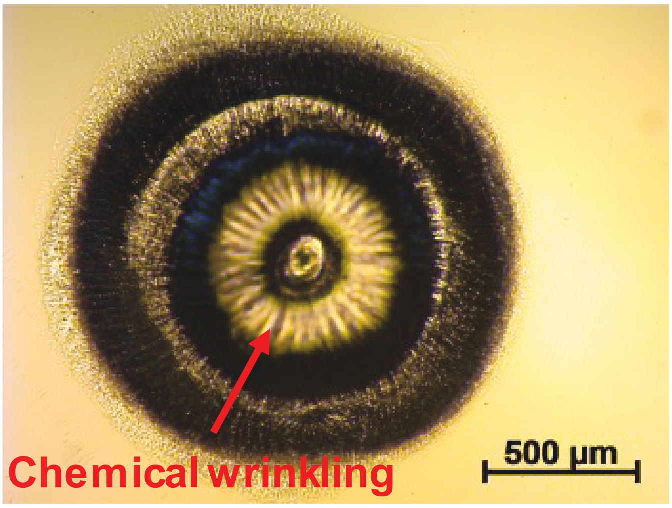

Figure 6. Machined surface for 2 M NaOH at 45 V at 50 ℃.

3.2 Effects of ions in the electrolyte

3.2.1 Spark color and surface damages in a pure electrolyte

Several ECDM experiments were done using acid, base, and neutral electrolytes. It was found that the spark color in ECDM is related to the ions in the electrolyte and varied with the change of electrolyte used. A list of different electrolytes and their corresponding sparking color is shown in Table 2. The sodium-based electrolyte has a sparking color of yellow in a wide range of pH values (i.e., from neutral to strong alkaline). Sodium related electrolyte discharges such as NaOH (strong alkaline), NaCl (neutral) and $NaNO_3$ (weak alkaline) were observed to spark in a yellow-orange color (Figure 7(a)). Potassium ions are observed sparking in a pink-purple glow (Figure 7 (b)). While hydrogen-based acid (e.g., H_2SO_4 and HCl) sparks in the color of blue and white (Figure 7c)). The color of the spark was also found to be the color of the sparking color of plasma vapor discharging similar to the vapor lamps (e.g., sodium vapor lamps glow in yellow-orange and potassium in pink-purple). This supports the statement in the previous section that the gas film formation includes vaporized electrolyte.

Table 2. A list of different 1 M electrolytes sparking color

Electrolyte	Color
NaOH	Orange
$NaNO_3$	Orange
NaCl	Orange
Na_2SO_4	Orange
$NiCl_2$	Orange
KOH	Pink
H_2SO_4	Blue
HCl	Blue

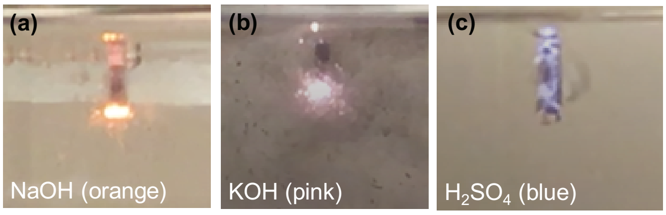

Figure 7. Sparking color difference observed with different 1 M electrolytes.

Scanning Electron Microscope (SEM) images of the machined surfaces are shown in Figure 8. Surface wrinkling was observed on surfaces machined with alkaline electrolytes (e.g., 2 M NaOH and KOH). These wrinkles were not seen on the surfaces machined with acid electrolyte. The presence of surface wrinkles in Figure 8 (a) and (b) are due to the chemical reactions of the hydroxyl ions of the alkaline electrolytes with the silicon of the glass workpiece [12]. In the experiment using 2 M H_2SO_4 as the electrolyte, the chemical damage did not occur due to the lack of OH ions. However, evidence of thermal damages including micro thermal cracks were observed in the machined surface (Figure 8(c)).

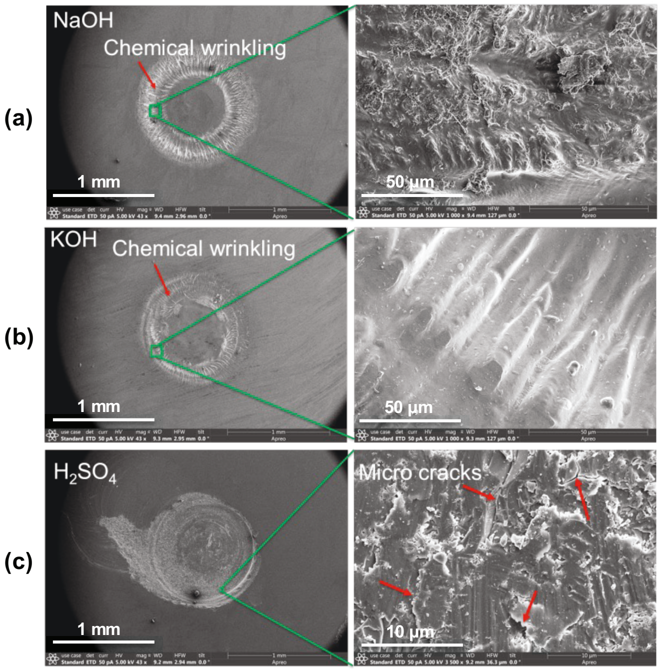

Figure 8. SEM images and section enlarged images for machining in different 2 M electrolyte (a) NaOH (b) KOH (c) H_2SO_4.

3.2.2 Spark color and surface damages in mixed electrolyte

ECDM with a mixture of more than one electrolyte results in the presence of multiple types of ions around the cathode. For example, when KOH and NaOH are mixed, both sodium and potassium ions will be present in the electrolyte. In an ECDM experiment performed at 45 V, the addition of a small amount of NaOH into KOH showed a pink glow in the sparks. When more NaOH was added in the electrolyte, the spark color changed to yellow-orange as shown in Figure 9. At a ratio of 1.6 M: 0.4 M KOH and NaOH mix, the pink sparks disappeared, and the orange sparks dominated.

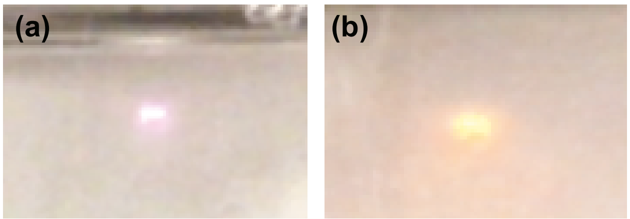

Figure 9. Comparison of the sparking color of (a) pure 2 M KOH and (b) mixed electrolyte of KOH and NaOH.

ECDM experiments using a mixture of acid and alkaline electrolytes were also tested, by adding NaOH into H_2SO_4. In this case, the yellow-orange sparks (from sodium ions) dominated before the electrolyte was neutralized. It is relatively difficult to quantify the ratio of sodium ions and H_2SO_4 as the neutralization process would reduce the concentration of both electrolytes and generation water which would further reduce the concentration. Moreover, the heat generated in the exothermic neutralization process can vaporize some of the electrolyte. For these reasons, Na_2SO_4 was added inside NaOH in the next experiment. At about 0.2 M concentration of Na_2SO_4, the color of the sparks become yellow as shown in Figure 10.

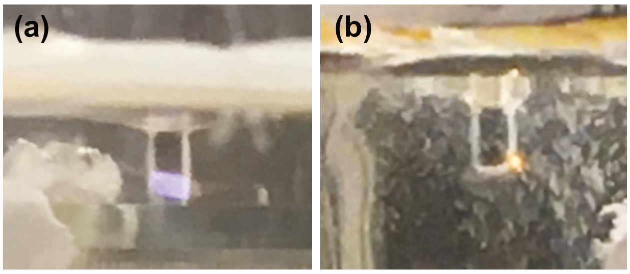

Figure 10. Comparison of the sparking color of (a) pure 2 M H_2SO_4 and (b) mixed electrolyte of H_2SO_4 and Na_2SO_4.

In addition to the ion concentration, the applied voltage also was found to influence the spark color as described below. An experiment was done using a mixed electrolyte (1 M NaOH and 1 M KOH) wherein voltage slightly higher than the critical voltage was initially applied and gradually increased, as shown in Figure 11. The results showed that at a lower voltage, most of the sparking is in pink color (i.e., potassium discharges). As the voltage increased, both pink and orange sparks were observed at the same time. At a higher voltage, the spark color becomes yellow-orange. A possible reason for these phenomena can be attributed to the energy (voltage) required for plasma discharging and to the differences in vaporizing temperature. Thus, it is evident that the spark color in ECDM is influenced by the ion concentration in the electrolyte and by the operating voltage.

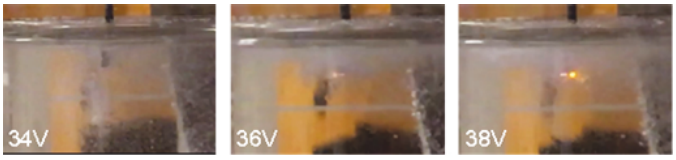

Figure 11. Images of the sparking from 34 V to 38 V. The sparks change from a pink color spark to yellow-orange as the voltage increases.

The observations made with current monitoring for each experiment including the pure electrolytes are summarized in Table 3. It can be seen that the maximum current is higher for KOH (e.g., 5.9 A) and NaOH (e.g., 6.5 A) when compared with the acids (e.g., 3.3 A). However, the sparking density (i.e., peaks per second) is higher for H_2SO_4 and HCl. On the other hand, the mixed electrolyte (i.e., H_2SO_4 + Na_2SO_4), shows a lower maximum current and also a lower spark density. When a small portion of Na_2SO_4 (0.2 M) was added, a significant drop in the mean current (0.1 A), maximum current (1.7 A), and peak density (45 per second) was noticed. When the ratio of Na_2SO_4 increased, the sparking energy also increased. Thus, with more Na_2SO_4 in the electrolyte, it is possible to increase the current values similar to that of pure NaOH electrolyte, and still avoid wrinkle formation by chemical etching by maintaining an acidic environment in the electrolyte. It should be noted that the mean current is the sum of the discharge current and the electrolysis current, the maximum current is related to the maximum energy that a spark would carry, and the peak density is the frequency of sparking. Therefore, from Table 3, it can be expected that ECDM with mixed electrolyte should result in minimum thermal damage and no surface wrinkling as lower peak current and spark density are observed for the electrolyte mixture of 1.2 M H_2SO_4 + 0.8 M Na_2SO_4.

Table 3. The current data for the different 2 M electrolytes used above.

Electrolyte	Mean current (*A*)	Maximum current (*A*)	Sparks peaks per second
2 M NaOH	0.42	5.94	1286
2 M KOH	0.67	6.47	1187
2 M H_2SO_4	0.55	3.44	1663
2 M HCl	0.40	3.31	1674
H_2SO_4 + Na_2SO_4			
1.8 M +0.2 M	0.10	1.72	45
1.6 M +0.4 M	0.26	3.87	385
1.2 M +0.8 M	0.54	6.10	822

3.3 Confirmation study

ECDM experiment with 0.2 M Na_2SO_4 and 1.8 M H_2SO_4 mixed electrolyte was performed to reduce the chemical and thermal damage in glass machining. SEM image of the machined surface shown in Figure 12 confirms that the chemical and thermal damages are mitigated when ECDM is performed using a mixed electrolyte.

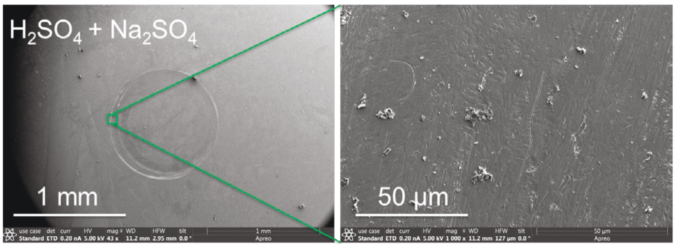

Figure 12. SEM images and section enlarged images for machining in 1.8M H_2SO_4 and 0.2M Na_2SO_4 electrolyte.

4. Conclusions

Following conclusions can be drawn based on the results from this study:

- Hydrogen bubbles resulting from electrolysis and vapors generated from heated electrolyte both contribute to the gas film formation in ECDM.
- The color of the spark can be adjusted by the ions in the electrolyte.
- In a mixture of electrolytes, the color can be controlled by changing the voltage and the ratio of electrolytes.
- The sparking energy is higher in ECDM with alkaline (KOH and NaOH) electrolytes, while the sparking density is higher in ECDM with acid (HCl and H_2SO_4) electrolytes.
- Formation of surface wrinkle formation in the glass is avoided when ECDM is performed in an acidic environment (i.e., lack of OH ions).
- The sparking density can be reduced by adding sodium ions into H_2SO_4 (i.e., a mixture of H_2SO_4 and Na_2SO_4). By adding a small portion of sodium ions, the sparking color would turn from blue to yellow-orange.
- Surface damages caused in the glass machining by ECDM by the thermal and chemical mechanisms are mitigated with the use of 1.2 M H_2SO_4 + 0.8 M Na_2SO_4 mixed electrolyte.

Acknowledgments

This material is based upon work supported by the National Science Foundation [Grant No. CMMI-1833112]. Any opinions, findings, and conclusions or recommendations expressed in this material are those of the author(s) and do not necessarily reflect the views of the National Science Foundation.

References

[1] Sundaram, M., and Rajurkar, K. P., 2010, "Electrical and electrochemical processes," Intelligent Energy Field Manufacturing and Interdisciplinary Process Innovations.

[2] Kurafuji, H., 1968, "Electrical Discharge Drilling of Glass-I," Annals of the CIRP, 16, p. 415.

[3] Jui, S. K., Kamaraj, A. B., and Sundaram, M. M., 2013, "High aspect ratio micromachining of glass by electrochemical discharge machining (ECDM)," Journal of Manufacturing Processes, 15(4), pp. 460-466.

[4] Langen, H., Breguet J, M., Bleuler, H., Ph, R., and Masuzawa, T., 1998, "Micro Electrochemical Discharge Machining of Glass," Int. J. elec. Mach., 3, pp. 65-69.

[5] Wüthrich, R., and Fascio, V., 2005, "Machining of non-conducting materials using electrochemical discharge phenomenon—an overview," International Journal of Machine Tools and Manufacture, 45(9), pp. 1095-1108.

[6] Wüthrich, R., and Bleuler, H., 2004, "A model for electrode effects using percolation theory," Electrochimica Acta, 49(9), pp. 1547-1554.

[7] Wüthrich, R., Fascio, V., and Bleuler, H., 2004, "A stochastic model for electrode effects," Electrochimica Acta, 49(22), pp. 4005-4010.

[8] Kolhekar, K. R., and Sundaram, M., 2018, "Study of gas film characterization and its effect in electrochemical discharge machining," Precision Engineering, 53, pp. 203-211.

[9] Allagui, A., and Wüthrich, R., 2009, "Gas film formation time and gas film life time during electrochemical discharge phenomenon," Electrochimica Acta, 54(23), pp. 5336-5343.

[10] Kellogg, H. H. J. J. o. t. e. s., 1950, "Anode effect in aqueous electrolysis," 97(4), pp. 133-142.

[11] Yerokhin, A. L., Nie, X., Leyland, A., Matthews, A., and Dowey, S. J., 1999, "Plasma electrolysis for surface engineering," Surface and Coatings Technology, 122(2), pp. 73-93.

[12] Kolhekar, K. R., and Sundaram, M., 2016, "A Study on the Effect of Electrolyte Concentration on Surface Integrity in Micro Electrochemical Discharge Machining," Procedia CIRP, 45, pp. 355-358.

[13] Harugade, M., Hargude, N., Shrotri, A., and Shinde, S., 2015, "A comparative study for selection of effective electrolyte solution for electrochemical discharge machining," International Journal of Mechanical Engineering & Technology (IJMET), 6, pp. 98-103.

[14] Sengupta, S. K., 1981, "The effect of electrolyte constituents on the onset and location of glow-discharge electrolysis," Journal of Electroanalytical Chemistry and Interfacial Electrochemistry, 127(1), pp. 263-265.

[15] Harugade, M., Kavade, M., and Hargude, N. J. I. J. M. C. E., 2013, "Effect of electrolyte solution on material removal rate in electrochemical discharge machining," pp. 1-8.

[16] Peng, W. Y., and Liao, Y. S., 2004, "Study of electrochemical discharge machining technology for slicing non-conductive brittle materials," Journal of Materials Processing Technology, 149(1), pp. 363-369.

[17] Raghuram, V., Pramila, T., Srinivasa, Y. G., and Narayanasamy, K., 1995, "Effect of the circuit parameters on the electrolytes in the electrochemical discharge phenomenon," Journal of Materials Processing Technology, 52(2), pp. 301-318.

[18] Sundaram, M., Chen, Y.-J., and Rajurkar, K., 2019, "Pulse electrochemical discharge machining of glass-fiber epoxy reinforced composite," CIRP Annals, 68(1), pp. 169-172.